Proceedings of the 17th World Congress
The International Federation of Automatic Control
Seoul, Korea, July 6-11, 2008

Calculating All K_P Admitting Stability of a PID Control Loop ⋆

Norbert Hohenbichler * **Dirk Abel** *

* *Institute of Automatic Control, RWTH Aachen University, 52056 Aachen, Germany (Tel: +49 241 80 27500; e-mail: secretary@irt.rwth-aachen.de).*

Abstract: To answer the outstanding question of the set of all stabilising PID controller parameters for a linear delay free system, the interval of all stabilising proportional gains K_P must be known, which admit stabilisation of the closed loop in addition with certain K_I and K_D. This paper presents a new algorithm for the numerical calculation of the stabilising K_P-interval, which entirely avoids gridding K_P. The algorithm is based on a new approach in analysing the motion of the stability boundaries in the (K_D, K_I)-plane, when K_P varies. A software tool implementing the algorithm in Matlab is available for download.

1. INTRODUCTION

The PID controller is without doubt the most common controller in industrial practice, and PID control pertains to the oldest control concepts. However, a generic algorithm to calculate the set of all stabilising controller parameters for an arbitrary linear system, even if it is delay free, is still missing. A key idea on the way to decoding the stable controller parameter space was that the stable region in the plane of (K_D, K_I) for fixed K_P consists of convex polygons, which was shown by an extension of the Hermite-Biehler-Theorem in Ho et al. (1998), in a simpler way by a D-Decomposition approach in Ackermann and Kaesbauer (2001, 2003) or by the Nyquist criterion in Söylemez et al. (2003). Consequently, the subproblem of calculating the stable region in the (K_D, K_I)-plane for given K_P can be considered as solved.

However, the question of choosing K_P in such a way that there is at least one stable (K_D, K_I)-plane polygon can still not be answered rigourously. Necessary conditions on the K_P-problem have been published in Söylemez et al. (2003) and Bajcinca (2006) which return K_P-intervals possibly being too large. The last reference mentions that one reason for being the intervals too large lies in the existence of so called *stability peaks* in the inner of the K_P-intervals where the stable region in the (K_D, K_I)-plane degenerates to a single point at a certain K_P.

This paper presents a new algorithm to calculate the stabilising K_P-interval rigorously, so that a gridding of K_P can be entirely avoided. A main point is the detection of stability peaks in the controller parameter space. It should not be concealed that the new algorithm does not apply for all arbitrary systems, however, testing the algorithm on a huge variety of systems showed that the conditions are not very restrictive.

⋆ This work was supported by the Deutsche Forschungsgemeinschaft (German Research Foundation) under project AB 65/2-1. The grant is thankfully acknowledged.

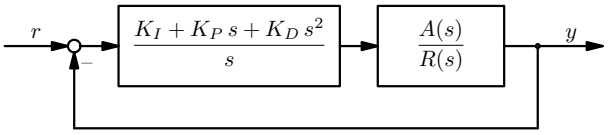

Fig. 1. PID control loop.

1.1 Problem Formulation

Consider a single control loop with an ideal PID controller and a linear delay free system (see Fig. 1), where K_I, K_P, K_D are the controller parameters and $A(s), R(s)$ are polynomials. The characteristic function of the loop is

$$P(s) = (K_I + K_P s + K_D s^2)\, A(s) + B(s) \quad , \quad (1)$$

with $B(s) = s\, R(s)$ and

$$A(s) = a_0 + a_1\, s + \ldots + a_m\, s^m, \quad a_m \neq 0 \; , \quad (2)$$

$$B(s) = \quad b_1\, s + \ldots + b_n\, s^n, \quad b_n \neq 0 \; . \quad (3)$$

The stated problem is to calculate the set of all K_P leading to a stable region in the (K_D, K_I)-plane.

1.2 D-Decomposition

In this paper, the D-Decomposition method is used to calculate the Hurwitz stable region in the controller parameter space. The method relies on the fact that the roots of the polynomial (1) move continuously when the controller parameters are changed continuously. Thus, a stable polynomial, whose roots all lie in the left half plane, becomes unstable if and only if at least one root crosses the imaginary axis. The corresponding parameter values of the root crossings form the *stability boundaries* in the parameter space, which can be classified into three cases: the *real root boundary (RRB)*, where a root crosses the imaginary axes at the origin, the *infinite root boundary (IRB)*, where a root leaves the LHP at infinity and the *complex root boundary (CRB)*, where a pair of complex conjugate roots crosses the imaginary axes. Additionally the moving direction of the roots can be calculated to mark the 'more' stable side of each boundary.

978-1-1234-7890-2/08/$20.00 © 2008 IFAC **10.3182/20080706-5-KR-1001.1270**

The stability boundaries separate different regions in the parameter space. To classify an entire region as stable it suffices to prove stability for one inner point (e.g. by the Hurwitz criterion).

1.3 The Stable Region in the (K_D, K_I, K_P)-Space

The key idea to obtain the stable region in the controller parameter space is to compose the three dimensional region by cutting it into (K_D, K_I)-plane slices by gridding K_P. For a fixed K_P^*, all stability boundaries in the (K_D, K_I)-plane are simple straight lines (without any approximations). Therefore, the stable regions are simple convex polygons. The advantage of knowing the set of all stabilising K_P a priori is that gridding can be reduced to this set.

1.4 Stability Boundaries in the (K_D, K_I)-Plane

Real and Infinite Root Boundary The RRB is given by the equation

$$P(0) = 0 \Leftrightarrow K_I = 0 \text{ if } a_0 \neq 0. \tag{4}$$

An IRB exists, when the leading coefficient of $P(s)$ depends on the controller parameter. This is only the case if $n = m + 2$. Then the IRB reads

$$K_D\, b_n + a_m = 0 \Leftrightarrow K_D = -\frac{b_n}{a_m}. \tag{5}$$

Complex Root Boundary A CRB in a (K_D, K_I)-plane for a fixed K_P^* is governed by the following system of two equations (for a proof, see Ackermann and Kaesbauer (2003); Bajcinca (2006))

$$f(\omega) - K_P^* = 0,\ \omega \in \mathbb{R}^+ , \tag{6}$$

$$K_I = K_D\omega^2 + g(\omega) \tag{7}$$

where $f(\omega)$ and $g(\omega)$ are the rational functions

$$f(\omega) = \frac{I_A R_B - R_A I_B}{\omega\,(R_A^2 + I_A^2)} , \tag{8}$$

$$g(\omega) = -\frac{R_A R_B + I_A I_B}{R_A^2 + I_A^2} , \tag{9}$$

and R and I denote the real and imaginary parts of A and B, respectively, at $s = \mathrm{j}\omega$.

The solutions of (6) are called *singular frequencies* ω_η. Note that depending on the number and the position of the extrema of $f(\omega)$ a unique index η can be assigned to a certain solution (see figure Fig. 7). Each ω_η corresponds to a straight CRB line, ruled by (7). That way, each CRB can be indexed by the index of its corresponding singular frequency as well.

Thus, all stability boundaries RRB, IRB and CRB are straight lines in the (K_D, K_I)-plane and partition the plane into convex polygons. As mentioned above, for each boundary line the 'more' stable side can be determined by calculating the moving direction of the root crossings. For the reason of brevity, details are omitted here, but Bajcinca (2006) can be used as reference. By classical stability tests of test points in the inner of the polygons the polygons can be rated stable or unstable.

Note that for certain K_P^* the polygons may degenerate to line sections (for a merging pair of singular frequencies at extrema of $f(\omega)$) or even to single points (at three-points, see following section), however, in this cases the degenerated polygons can still be classified as limit stable or unstable.

1.5 The Stabilising K_P-Interval

The remaining question is, which K_P^* should be chosen to get at least one stable polygon in the (K_D, K_I)-plane. In other words, the interval of stabilising K_P is to be determined.

Necessary Condition A necessary condition is given in Bajcinca (2006) as theorem 2. The theorem states a minimal number of singular frequencies at a certain K_P^*. Note that depending on the number of extrema of $f(\omega)$ and the function values of $f(\omega)$ at the extrema, the number of singular frequencies may be different for different K_P^* (see Fig. 7).

Assume that $A(s)$ has no zeros on the imaginary axis. The necessary stability condition for a K_P^* is that the number [1] Z of singular frequencies $\omega_g \in \mathbb{R}^+$ suffices

$$Z \geq \left\lfloor \frac{n' - m + 2p - 1}{2} \right\rfloor , \tag{10}$$

where $n' = \max(n, m+2)$ is the degree of polynomial (1), p is the number of zeros of $A(s)$ in the right half plane and $\lfloor\cdot\rfloor$ denotes the floor function. For the proof and extensions to the case of $A(s)$ having zeros on the imaginary axis see Bajcinca (2006).

Stability peaks In two different cases, the theorem leads to K_P-intervals which actually do not belong to the set of all stabilising K_P: Either a K_P-interval, which possesses a number of singular frequencies reaching the required minimal number, is completely unstable, or the stability property changes in the middle of such a K_P-interval. The latter case occurs if there exist so called *stability peaks* in the controller parameter space, where a stable (K_D, K_I)-plane polygon reduces to a single point for a certain K_P (see Bajcinca (2006)).

The goal of this paper is to check if there exist stability peaks, and if so, to locate the stability peaks in the (K_D, K_I, K_P)-space. After dividing the K_P-intervals at the K_P-values of all stability peaks, the question of the stabilising K_P-interval can be solved with sufficiency by calculating the stable (K_D, K_I)-plane polygons at an arbitrary K_P in the interval.

Obviously, a stability peak exists, if and only if

- three root boundaries (RRB, IRB or CRBs) coincide in one point (this point is called a *three-point*), and
- the three-point limits a stable region in the controller parameter space.

2. K_P-INTERVALS AND BOUNDARY COMBINATIONS

The first step of the proposed algorithm is the definition of intervals of K_P in which some functions of the singular

[1] Note that in this paper $\omega = 0$ is not counted as singular frequency.

frequencies behave monotonically such that interval approximations can be made.

Let Ω^{ex} be the set of all frequencies ω where the function $f(\omega)$ (8), $K_D^c(\omega)$ (15) or $h(\omega)$ (41) possesses a local extremum with $\omega \in \mathbb{R}^+$. The limits of the K_P-intervals are defined as

$$\{f(\omega) \mid \omega \in \Omega^{\text{ex}}\} \ . \tag{11}$$

The definition of the K_P-intervals ensures that $f(\omega_\eta)$, $K_D^c(\omega_\eta)$ and $h(\omega_\eta)$ vary monotonically for each singular frequency ω_η, when K_P is varied monotonically in a K_P-interval. The monotonicity properties will be needed in the following sections.

The K_P-interval defines a frequency interval

$$[\omega_\eta^-, \omega_\eta^+],\ \omega_\eta^- < \omega_\eta^+ \ , \tag{12}$$

in which the singular frequency with index η resides (see Fig. 7).

To search for three-points, all possible combinations of three root boundaries need to be checked for each K_P-interval. Remember that individual indices are yet assigned to CRBs. To bring the RRB and the IRB into the same framework, the following arbitrary indices are assigned to these kind of root boundaries:

- $\eta = -1$ for the RRB,
- $\eta = -2$ for the IRB, if it exists.

The set of all combinations of three root boundaries in a certain K_P-interval is denoted as

$$\hat{I} := \{I_\nu := \{i, j, k\}\} \ , \tag{13}$$

where i, j, k cycle through all combinations of three different indices of the K_P-interval. I_ν represents a certain combination of three root boundary indices.

3. ROOT BOUNDARY MOTION

To find the three-points, the motion of the CRB lines in the (K_D, K_I)-plane is analysed for varying K_P and ω, respectively. The motion w.r.t. ω described by (7) can be split up into a translation and a rotation part by the help of an instantaneous center of rotation (i.c.r.).

At the i.c.r. the movement is a pure rotation. As the derivative of (7) w.r.t. ω

$$\frac{\partial K_I}{\partial \omega} = 2K_D\omega + g'(\omega) \ , \tag{14}$$

vanishes at the CRB line itself for

$$K_D^c(\omega) = -\frac{g'(\omega)}{2\omega} \ , \tag{15}$$

$$K_I^c(\omega) = -\frac{\omega g'(\omega)}{2} + g(\omega) \ , \tag{16}$$

the i.c.r. always lies on the CRB itself and is desribed by the coordinates $K_D^c(\omega)$ and $K_I^c(\omega)$.

The CRB line is then described in parametric form as

$$K_D = K_D^c(\omega) + \lambda\cos(\alpha) \tag{17}$$

$$K_I = K_I^c(\omega) + \lambda\sin(\alpha) \tag{18}$$

$$\alpha = \arctan(\omega^2) \tag{19}$$

with the parameter $\lambda \in \mathbb{R}$.

The following important properties of the i.c.r. trajectory w.r.t. ω can be summarised:

Table 1. Inhibited angle interval Γ_η depending on the root boundary type and the stable side.

Γ_η	Type	Stable Side at
$[\alpha_\eta^-, \alpha_\eta^+ + \pi]$	CRB	small K_D
$[0, \alpha_\eta^+] \cup [\alpha_\eta^- + \pi, 2\pi]$	CRB	large K_D
$[0, \pi]$	RRB	small K_I
$[\pi, 2\pi]$	RRB	large K_I
$[\pi/2, 3\pi/2]$	IRB	large K_D
$[0, \pi/2] \cup [3\pi/2, 2\pi]$	IRB	small K_D

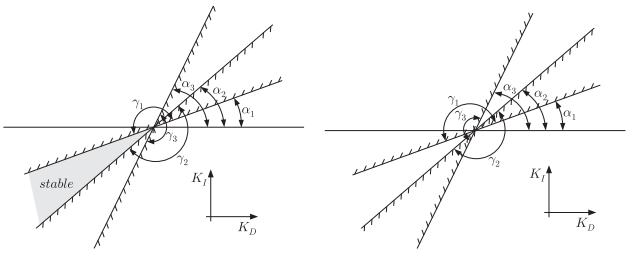

Fig. 2. Two different three-points as the intersection of three CRBs 1,2,3. Left: Not stability critical three-point. Right: Stability critical three-point.

- The i.c.r. always lies on the CRB itself and moves in direction of α when ω is varied.
- The i.c.r. trajectory is left-curved w.r.t. rising ω, because of (19),
- The i.c.r. trajectory exhibits reversal points where $K_D^c(\omega)$ possesses a local extremum.

4. NECESSARY CONDITIONS FOR THREE-POINTS

This sections derives necessary conditions for the existence of three-points of a certain combination I_ν. The conditions serve to discard a huge amount of combinations which will not lead to stability peaks.

4.1 Inhibited Angle Range

Assume that a certain combination I_ν possesses a three-point. It can be observed that the three-point may be stability critical or not (see Fig. 2), depending on the angles α_η and the stable sides of the boundary lines.

The inhibited angle γ_η of a stability boundary is defined as depicted in Fig. 2. When K_P is varying in its interval, each CRB line angle α_η moves in an interval $[\alpha_\eta^-, \alpha_\eta^+]$ with $\alpha_\eta^- = \arctan((\omega_\eta^-)^2)$ and $\alpha_\eta^+ = \arctan((\omega_\eta^+)^2)$, so the inhibited angle γ_η traverses the interval Γ_η given in Table 1. The intervals for RRBs and IRBs are denoted as well.

Obviously, if the union of all intervals Γ_η of a combination I_ν does not cover the entire circle,

$$\bigcup_{\eta \in I_\nu} \Gamma_\eta \neq [0, 2\pi] \ , \tag{20}$$

the combination I_ν will not lead to a stability critical three-point and can be discarded.

4.2 Root Boundary Envelopes

For each root boundary η an envelope of the root boundary movement can be given. The envelope describes the region

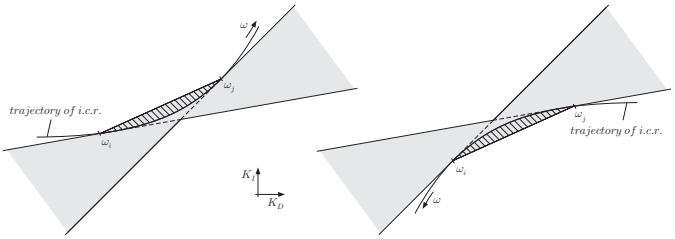

Fig. 3. Envelopes of a CRB for increasing (left) or decreasing $K_D^c(\omega)$ (right). The hatched region represents the conservatism added by substituting the i.c.r.-trajectory by a line.

in the (K_D, K_I)-plane which is traversed by the root boundary when K_P is varied in its interval.

Considering the properties of the i.c.r.-trajectory and the fact that in a K_P-interval $K_D^c(\omega)$ varies monotonically, the traversed area of a CRB is bounded by five elements which restrict a non-convex and non-bounded region (see Fig. 3):

(1) The part of the i.c.r.-trajectory between ω_η^- and ω_η^+.
(2) Two rays as elongations of the i.c.r-trajectory at both ends, with angles $\arctan((\omega_\eta^-)^2)$ and $\arctan((\omega_\eta^+)^2)$.
(3) Two rays which start at the intersection point of the CRBs at ω_η^- and ω_η^+, with angles $\arctan((\omega_\eta^-)^2)$ and $\arctan((\omega_\eta^+)^2)$.

By substituting part 1 by a line connecting the points of the i.c.r-trajectory at ω_η^- and ω_η^+, a conservative envelope of the traversed area can be derived. It is a non-convex and non-bounded polygon which can be handled much simpler by computer algorithms than the exact region. The envelope boundaries of a CRB can be described by the following linear inequalities:

If $K_D^c(\omega)$ is increasing in $[\omega_\eta^-\ \omega_\eta^+]$:

$$bl_\eta^1 = \{\{K_D, K_I\} \mid K_I \le c\,K_D + d\} \tag{21}$$
$$bl_\eta^2 = \{\{K_D, K_I\} \mid K_I \le (\omega_\eta^-)^2 K_D + g(\omega_\eta^-)\} \tag{22}$$
$$bl_\eta^3 = \{\{K_D, K_I\} \mid K_I \le (\omega_\eta^+)^2 K_D + g(\omega_\eta^+)\} \tag{23}$$
$$br_\eta^1 = \{\{K_D, K_I\} \mid K_I \ge (\omega_\eta^-)^2 K_D + g(\omega_\eta^-)\} \tag{24}$$
$$br_\eta^2 = \{\{K_D, K_I\} \mid K_I \ge (\omega_\eta^+)^2 K_D + g(\omega_\eta^+)\} \tag{25}$$

If $K_D^c(\omega)$ is decreasing in $[\omega_\eta^-\ \omega_\eta^+]$:

$$br_\eta^1 = \{\{K_D, K_I\} \mid K_I \ge c\,K_D + d\} \tag{26}$$
$$br_\eta^2 = \{\{K_D, K_I\} \mid K_I \ge (\omega_\eta^-)^2 K_D + g(\omega_\eta^-)\} \tag{27}$$
$$br_\eta^3 = \{\{K_D, K_I\} \mid K_I \ge (\omega_\eta^+)^2 K_D + g(\omega_\eta^+)\} \tag{28}$$
$$bl_\eta^1 = \{\{K_D, K_I\} \mid K_I \le (\omega_\eta^-)^2 K_D + g(\omega_\eta^-)\} \tag{29}$$
$$bl_\eta^2 = \{\{K_D, K_I\} \mid K_I \le (\omega_\eta^+)^2 K_D + g(\omega_\eta^+)\}\ , \tag{30}$$

where

$$c = \frac{K_I^c(\omega_\eta^+) - K_I^c(\omega_\eta^-)}{K_D^c(\omega_\eta^+) - K_D^c(\omega_\eta^-)}\ , \tag{31}$$

$$d = \frac{K_D^c(\omega_\eta^+)K_I^c(\omega_\eta^-) - K_D^c(\omega_\eta^-)K_I^c(\omega_\eta^+)}{K_D^c(\omega_\eta^+) - K_D^c(\omega_\eta^-)}\ . \tag{32}$$

The envelope $\mathrm{env}(\eta)$ for a CRB η is the intersection of the union of all left boundaries bl and the union of all right boundaries br

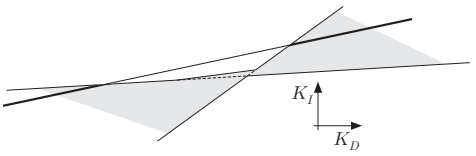

Fig. 4. Intersection of a line with a CRB envelope.

$$\mathrm{env}(\eta) = \left(\bigcup_\kappa bl_\eta^\kappa\right) \cap \left(\bigcup_\kappa br_\eta^\kappa\right)\ . \tag{33}$$

As the RRB and IRB do not depend on K_P, its envelopes $\mathrm{env}(\eta) = b_\eta$ are the stability boundaries (4,5) themselves.

4.3 Three-Point Regions

A necessary condition for the existence of a three-point is that the envelopes of a combination I_ν possess a non-empty intersection, which will be called a *three-point region* $\mathrm{tpr}(I_\nu)$.

The intersection of a combination I_ν (e.g., let i, j be CRBs and k a RRB) is

$$\mathrm{tpr}(I_\nu) = \mathrm{env}(i) \cap \mathrm{env}(j) \cap \mathrm{env}(k) = \left(\bigcup_{\kappa_1} bl_i^{\kappa_1}\right) \cap \left(\bigcup_{\kappa_2} br_i^{\kappa_2}\right) \cap \left(\bigcup_{\kappa_3} bl_j^{\kappa_3}\right) \cap \left(\bigcup_{\kappa_4} br_j^{\kappa_4}\right) \cap b_k = \bigcup_{\kappa_1,\kappa_2,\kappa_3,\kappa_4} \left(bl_i^{\kappa_1} \cap br_i^{\kappa_2} \cap bl_j^{\kappa_3} \cap br_j^{\kappa_4} \cap b_k\right)\ , \tag{34}$$

where $\kappa_1, \kappa_2, \kappa_3, \kappa_4$ cycle through all combinations of the boundary elements of the CRB envelopes.

By (34), handling of the non-bounded envelopes can be circumvented by calculating the intersection of all combinations of all left and right boundaries of the CRB envelopes and the RRB and IRB boundaries, respectively. Each intersection will be a convex polygon as it results from a system of linear inequalities.

It can be shown by a short proof of contradiction that $\mathrm{tpr}(I_\nu)$ is bounded and consists of at most one connected region: Consider the intersection of two CRB envelopes. Now from the first envelope an arbitrary CRB is taken and intersected with the second envelope (see Fig. 4). If there are more than one unconnected intersections or if there is an unbounded intersection, the slope of the CRB has to be between the slopes of the boundary elements of the second envelope. As the slopes are ω_η^2, the frequency ranges of the CRBs have to intersect. However, this is a contradiction to the definition of the K_P-intervals, which implies that the frequency ranges are seperated. This holds for all CRBs in the first envelope and so for the whole intersection of both envelopes and obviously also for the intersection of three envelopes. Note that the proof extends to RRB and IRB envelopes as well.

Note that by uniting bounded convex polygons, a bounded non-convex polygon may result. As the three-point region is always a single connected region the non-convex polygon may be approximated by a convex hull polygon without adding too much conservatism.

5. UNIQUENESS OF A THREE-POINT

With means of the necessary conditions in the last section, many combinations I_ν can be discarded when searching for a stability peak. However, if a non-empty three-point region is found, it is important to determine wether the region contains a unique three-point. For that reason, the motion of intersection points of the root boundaries for a variation of K_P is further studied.

5.1 Kinematics of Intersection Points

In this section the intersection point motion of two root boundaries is calculated by applying basic kinematics (see Fig. 5). To describe the motion, a velocity vector is defined as the following partials

$$\boldsymbol{v} = \begin{pmatrix} \frac{\partial K_D}{\partial K_P} & \frac{\partial K_I}{\partial K_P} \end{pmatrix}^T , \tag{35}$$

which represents the movement of a certain point in the (K_D, K_I)-plane when K_P is varied.

First, the intersection point of two CRBs i and j is considered. Remember that the i.c.r. always moves in the direction of its corresponding CRB angle α_η (see $\boldsymbol{v}_{i/j}$ in Fig. 5). Thus, the normal velocity at the intersection point of the CRB η only depends on the rate of change of α_η

$$\boldsymbol{v}_\eta^r = a_\eta \frac{\partial \alpha_\eta}{\partial K_P} \begin{pmatrix} -\sin\alpha_\eta \\ \cos\alpha_\eta \end{pmatrix}, \ \eta = i, j \ , \tag{36}$$

where a_η is the distance from the i.c.r. η to the intersection point xp. a_η is defined positive when the intersection point is at the side of larger K_D/K_I w.r.t. to the i.c.r. η. Otherwise a_η is negative.

Only the normal velocities $\boldsymbol{v}_\eta^r$ influence the intersection point movement. The velocity of the intersection point $\boldsymbol{v}_{ij}^{\text{xp}}$ is the sum of both normal velocities projected onto the other CRB, as depicted in Fig. 5

$$\boldsymbol{v}_i^{\text{xp}} = \frac{|\boldsymbol{v}_i^r|}{\cos\alpha_i \, \sin^2\alpha_i + \sin\alpha_i \, \sin^2\alpha_j} \begin{pmatrix} \cos\alpha_j \\ \sin\alpha_j \end{pmatrix} , \tag{37}$$

$$\boldsymbol{v}_j^{\text{xp}} = \frac{|\boldsymbol{v}_j^r|}{\cos\alpha_j \, \sin^2\alpha_j + \sin\alpha_j \, \sin^2\alpha_i} \begin{pmatrix} \cos\alpha_i \\ \sin\alpha_i \end{pmatrix} , \tag{38}$$

$$\boldsymbol{v}_{ij}^{\text{xp}} = \boldsymbol{v}_i^{\text{xp}} + \boldsymbol{v}_j^{\text{xp}} \ . \tag{39}$$

With $\alpha = \arctan(\omega^2)$, $\frac{\partial \alpha}{\partial K_P} = \frac{2\omega}{f'(\omega)(1+\omega^4)}$ and some trigonometric simplifications, the velocity of the intersection point can be described as

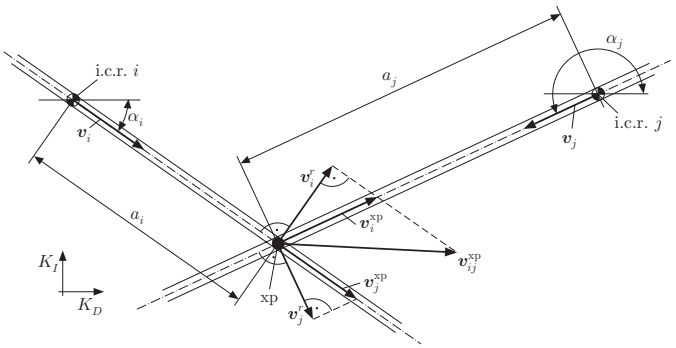

Fig. 5. Kinematics of the intersection of CRBs i and j.

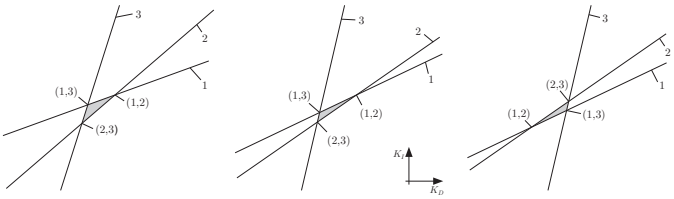

a) Original situation b) Vertices stay at same side. c) Vertices change side.

Fig. 6. Enclosed triangle of a combination I_ν at K_P-interval limits. a) First K_P limit. b) Second K_P limit, where the vertices stay at the same side of the opposite edges. c) Second K_P limit, where the vertices change the side w.r.t. the opposite edges.

$$\boldsymbol{v}_{ij}^{\text{xp}} = \frac{1}{\omega_j^2 - \omega_i^2} \begin{pmatrix} h(\omega_i)\, a_i - h(\omega_j)\, a_j \\ \omega_j^2\, h(\omega_i)\, a_i - \omega_i^2\, h(\omega_j)\, a_j \end{pmatrix} , \tag{40}$$

where

$$h(\omega) = \frac{2\omega}{f'(\omega)\sqrt{1+\omega^4}} \ . \tag{41}$$

Note that the movement of the intersection point of a CRB and a RRB or an IRB can be calculated similarly and is omitted here for the reason of brevity.

5.2 Unique Solution Condition of a Three-Point

No more than one Solution By equation (40), velocity intervals of the intersection points of a combination I_ν can be derived. As three-points only reside in $\text{tpr}(I_\nu)$, an interval for the distances a_η can be estimated as $[a_\eta^-, a_\eta^+]$. In the K_P-interval, $h(\omega)$ varies monotonically when ω_η varies monotonically in (12). Thus, by applying basic interval algebra on the equation (40), intervals for both coordinates of the intersection point velocity

$$[\boldsymbol{v}_{ij-}^{\text{xp}}, \boldsymbol{v}_{ij+}^{\text{xp}}] \tag{42}$$

can be given.

A sufficient condition to check if the combination I_ν possesses no more than one three-point in the K_P-interval can be derived from the intervals

$$[\boldsymbol{v}_{ij-}^{\text{xp}}, \boldsymbol{v}_{ij+}^{\text{xp}}] \tag{43}$$

$$[\boldsymbol{v}_{ik-}^{\text{xp}}, \boldsymbol{v}_{ik+}^{\text{xp}}] \tag{44}$$

$$[\boldsymbol{v}_{jk-}^{\text{xp}}, \boldsymbol{v}_{jk+}^{\text{xp}}] \quad i, j, k \in I_\nu \ . \tag{45}$$

If the K_D-coordinates or the K_I-coordinates of the intervals (43,44,45) do not intersect this condition is fulfilled. To prove this proposition the reader may consider that the root boundaries i, j, k coincide in the point $[K_D^*,\ K_I^*]$. If the velocity coordinates do not intersect, the three intersection points diverge in the (K_D, K_I)-plane.

One Unique Solution If the intersection point velocities do not intersect, the enclosed triangle can be examined at the K_P-interval limits to decide if the combination I_ν possesses a unique or no three-point.

Obviously, there exists a unique three-point if and only if the vertices of the enclosed triangle of the combination I_ν change the side w.r.t. to their opposite edges, when K_P jumps from the first to the second limit of the K_P-interval (see Fig. 6).

6. NUMERICAL SOLUTION

If the existence and the uniqueness of a three-point in a K_P-interval is shown by the proposed means, the following nonlinear system (here given for the combination of three CRBs, all other cases are similar) of six equations can be safely solved by standard numerical algorithms

$$\begin{aligned} K_I^{\text{xp}} - K_D^{\text{xp}}\omega_\eta^2 - g(\omega_\eta) &= 0 \ , \\ f(\omega_\eta) - K_P^{\text{xp}} &= 0 \ , \quad \eta = i,j,k \ , \end{aligned} \tag{46}$$

with the six unknown variables K_I^{xp}, K_D^{xp}, K_P^{xp}, ω_i, ω_j and ω_k. As initial conditions for the numerical search, mean values of the $\text{tpr}(I_\nu)$, the K_P-interval and the singular frequency intervals (12) can be used.

7. PROPOSED ALGORITHM

The complete algorithms consists of the following steps:

(1) Define K_P-intervals (see Section 2).
(2) Apply necessary condition in Section 1.5 on all K_P-intervals: Discard all intervals that possess a lower number of singular frequencies than required.
(3) For all remaining K_P-intervals:
  (a) For all combinations $I_\nu \in \hat{I}$: Check inhibited angle range (see Section 4.1) and discard the combinations I_ν which cannot lead to a stability peak.
  (b) For all remaining combinations I_ν: Check, if combination I_ν possesses a non-empty three-point region $\text{tpr}(I_\nu)$ (see Section 4). If no three-point region exists or all combinations I_ν are discarded: Jump to next K_P-interval.
  (c) For all three-point regions $\text{tpr}(I_\nu)$: Check if the intersection point velocities do not intersect to guarantee that there is no more than one three-point in the $\text{tpr}(I_\nu)$ (see Section 5.2). If yes: Proceed. If no: This case can not be handled by the algorithm.
  (d) For all three-point regions $\text{tpr}(I_\nu)$: Check if the order of the enclosed polygon vertices of the combination I_ν changes at the K_P-interval limits to check if there exists a unique three-point (see Section 5.2). If not, discard the three-point region $\text{tpr}(I_\nu)$.
  (e) For all remaining three-point regions $\text{tpr}(I_\nu)$: Perform numerical search for a solution of equation system (46) (see Section 6) in $\text{tpr}(I_\nu)$. Divide current K_P-interval into two intervals at the K_P-value of the found solution.
(4) For all K_P-intervals: Evaluate stability of the K_P-interval by inspecting the number of stable polygons in the (K_D, K_I)-plane for an arbitrary K_P^* in the interval.
(5) Join all stabilising K_P-intervals to the searched set of all stabilising K_P.

8. EXAMPLE AND SOFTWARE TOOL

The following example out of Bajcinca (2006) illustrates the proposed algorithm. Let the polynomials be

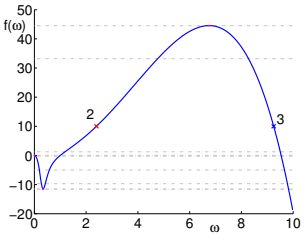

Fig. 7. Function $f(\omega)$ (solid), K_P-interval limits (dashed) and singular frequencies with ids 2 and 3 for a $K_P^* = 10$.

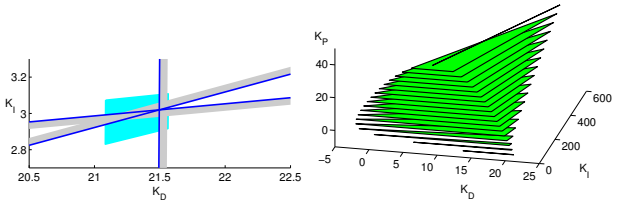

Fig. 8. Left: The CRBs at $K_P = -9.00238$ and the three-point region of indices $1, 2, 3$ in the K_P-interval $(-9.673227, -5.027932)$. Right: The space of all stabilising controller parameters.

$$A(s) = 1890\,s^2 + 658\,s + 215 \tag{47}$$

$$\begin{aligned} B(s) = {} & s^8 + 1032/25\,s^7 + 6175327/10000\,s^6 + \\ & 98620159/25000\,s^5 + 92785263/10000\,s^4 + \\ & 97588159/25000\,s^3 + 5413746/625\,s^2 \ . \end{aligned} \tag{48}$$

The monotonicity conditions in Section 2 lead to 11 K_P-intervals. The function $f(\omega)$ and the K_P-interval limits are depicted in Fig. 7. Only the combination $\nu = \{1, 2, 3\}$ in the K_P-interval $(-9.673227, -5.027932)$ returns a $\text{tpr}(\nu)$ (see Fig. 8). The $\text{tpr}(\nu)$ satisfies the uniqueness condition in Section 5.2. The numerical search returns the new K_P limit as -9.00238. Continuing the algorithm the searched interval of all stabilising K_P for the example reveals to be $(-9.00238, 44.54973)$.

A software tool based on Matlab, which performs all steps calculating the space of the stabilising controller parameters automatically, is available for download at http://www.irt.rwth-aachen.de/pidrobust.

REFERENCES

J. Ackermann and D. Kaesbauer. Design of robust PID controllers. In *Proceedings of European Control Conference*, Porto, 2001.

J. Ackermann and D. Kaesbauer. Stable polyhedra in parameter space. *Automatica*, 39(5):937–943, 2003.

N. Bajcinca. Design of robust PID controllers using decoupling at singular frequencies. *Automatica*, 42: 1943–1949, 2006.

M. Ho, A. Datta, and S. Bhattacharayya. Design of P, PI and PID controller for interval plants. In *Proc. American Control Conference*, pages 2496–2501, Philadelphia, 1998.

M. T. Söylemez, M. Munro, and H. Baki. Fast calculation of stabilizing PID controllers. *Automatica*, 39:121–126, 2003.